Vol. 91 (1997) *ACTA PHYSICA POLONICA A* No. 2

Proceedings of the European Conference "Physics of Magnetism 96", Poznań 1996

TEMPERATURE DEPENDENCE OF MAGNETIC INELASTIC NEUTRON SCATTERING IN Mn(12%Ge) ALLOY

J. JANKOWSKA-KISIELIŃSKA, K. MIKKE, J.J. MILCZAREK

Institute of Atomic Energy, Świerk, 05-400 Otwock, Poland

B. HENNION

Laboratoire Léon Brillouin, CEN Saclay, France

AND V.A. UDOVENKO

Institute of Physical Metallurgy, Moscow, Russia

A systematic study of temperature dependence of magnetic inelastic neutron scattering for itinerant antiferromagnet Mn(12%Ge) is presented. At low temperatures the experimental data are well described in terms of damped spin waves. This description becomes insufficient at least 150 K below T_N. In the temperature range 200–400 K the integrated intensity of distribution for energy transfer 13 THz increases by one third and the shape of the deconvoluted neutron scattering cross-section changes. These changes suggest that *ca.* 200 K below T_N an additional contribution to the inelastic neutron scattering starts to appear and that its origin is different from spin waves.

PACS numbers: 75.30.Ds, 75.50.Ee

The magnetic excitations in itinerant antiferromagnets are not yet satisfactorily understood. In particular more detailed studies of their temperature dependence are needed. The aim of our experiment was to study the evolution of the neutron scattering by spin waves at low temperature into the paramagnetic scattering above T_N.

The crystal structure of the γ-Mn alloys with high manganese concentration (fcc in the paramagnetic phase) becomes tetragonal with $c < a$ in the antiferromagnetic (AF) phase. Many alloys with lower manganese concentration remain fcc in the AF phase. In some narrow concentration region (different for different diluents) two other crystal structures: orthorhombic and tetragonal with $c > a$ appear in the AF phase. The composition of the investigated alloy is close to the composition for the tricritical point for paramagnetic fcc, AF tetragonal and AF

orthorhombic phases. At room temperature it is antiferromagnet with tetragonal structure. Tetragonal deformation is $1 - c/a = 0.013$. The estimated Néel temperature is 470–490 K. The investigated sample is a polydomain single-crystal with the mosaic spread *ca.* 2°.

The measurements were performed using a 3-axis neutron spectrometer at the Orphèe reactor in LLB CEN Saclay. The scattered neutron energy was constant $E_f = 3.55$ THz. The horizontal collimations starting from the reactor core were 26′–30′–60′–60′. The intensity distributions versus momentum transfer for energy transfers 5, 8 and 13 THz were measured in the temperature range 19–600 K. At temperatures 19 and 295 K additional distributions were measured to obtain more complete data on the dispersion relation. The energy distribution of the incoherent scattering was measured far from the Brillouin zone (BZ) center at 19 K. It was used to estimate the incoherent scattering at higher temperatures. Examples of the intensity distributions measured at 19 K are presented in Fig. 1. The solid lines in the figure show the results of the computed convolution of the spectrometer resolution function with the neutron scattering cross-section for the damped oscillator model. The dashed lines indicate the background plus incoherent scattering level.

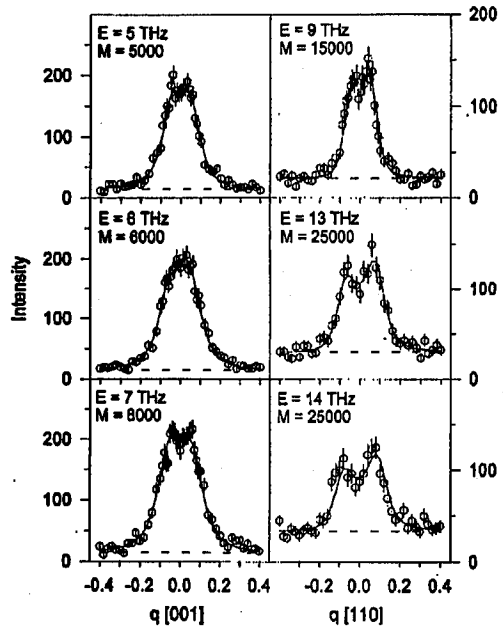

Fig. 1. The intensity distributions versus momentum transfer for energy transfers 5, 6 and 7 THz measured in [001] direction and for 9, 13 and 14 THz — in [110] direction at 19 K.

For data analysis below T_N we used the neutron scattering cross-section for damped spin waves. Two formulae were used: the one for itinerant antiferromagnet (Liu [1], Sato and Maki [2]), which reads as follows:

$$\frac{\mathrm{d}^2\sigma}{\mathrm{d}\Omega \mathrm{d}E} \simeq F^2(Q)[n(E)+1]\frac{\Gamma E}{(E^2-E_q^2)^2+\Gamma^2E^2} \tag{1}$$

and another one, for a damped harmonic oscillator (used for Mn(10%Cu) [3]):

$$\frac{\mathrm{d}^2}{\mathrm{d}\Omega \mathrm{d}E} \simeq F^2(Q)[n(E)+1]\frac{\Gamma E}{(E^2-E_q^2)^2+\Gamma^2E^2}\frac{\kappa^2}{\kappa^2+q^2}, \tag{2}$$

where $n(E)$ is the population factor, $F(Q)$ — magnetic form factor, κ — inverse correlation range, q — momentum reduced to the magnetic BZ. The spin wave energy follows the formula

$$E_q^2 = v^2q^2 + E_g^2, \tag{3}$$

where v is the spin wave velocity and E_g — the energy gap in the spin wave spectrum. The spin wave damping parameter Γ in these alloys has a linear dependence on the momentum q

$$\Gamma = \Gamma_0 + \Gamma_1 q. \tag{4}$$

The parameters of the dispersion relation v and E_g and of the damping Γ_1 were obtained by computer fitting of the intensity distributions. Goodness of fits for 19 K is slightly better for the second formula. The obtained shape of the cross-section is nearly independent on the used formula. The mean values of parameters for the first formula are: $v = 48 \pm 6$ THz Å, $E_g = 1.96 \pm 0.04$ THz and $\Gamma_1 = 38 \pm 13$ THz Å. For the second formula the mean values are $v = 54 \pm 4$ THz Å and $\Gamma_1 = 39 \pm 20$ THz Å for $\kappa = 0.1$ Å^{-1}. At temperatures 100 and 200 K only 3 scans were performed for energy transfers 5, 8 and 13 THz. The obtained values of the parameters differ slightly, the velocity decreases and the damping increases. At 300–350 K a sudden increase in damping parameter is observed. The increase of damping is, however, not sufficient to describe the change of the shape of the measured distributions in terms of any of the above formulae. The quality of fits decreases drastically; the parameter χ^2 is smaller than 2 only for 13 and 14 THz. Above 300 K fits for all measured distributions are rather poor (χ^2 usually bigger than 1.5). Above T_N the analysis in terms of paramagnetic fluctuations [4] is not yet completed.

The integrated intensity of the distribution versus momentum for energy 13 THz divided by the population factor is shown in Fig. 2. One observes the increase in the integrated intensity by about one third in the temperature range 200–375 K. Above 400 K there is a slow decrease. The main change takes place in a rather narrow temperature range and, surprisingly, much below T_N. The deconvoluted neutron scattering cross-section derived using the first formula from distributions for 13 THz for different temperatures is shown in Fig. 3. The shapes for 19 and 200 K are very similar, for 350 and 400 K they are also similar to each other but quite different from the first two. The maxima are shifted towards the center, the distributions are broader and they go very slowly to 0 for a larger q. The shape for 300 K is intermediate. The changes in the intensity and shape of the

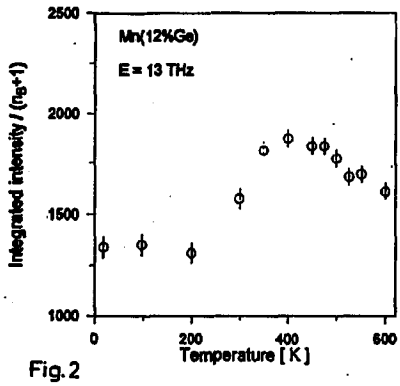

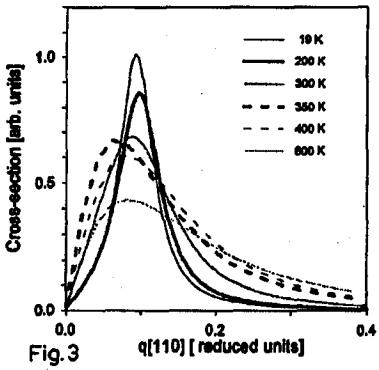

Fig. 2. The temperature dependence of the integrated intensity of the distribution for energy transfer 13 THz corrected for the background, the incoherent scattering and the population factor.

Fig. 3 The neutron scattering cross-section divided by the population factor, derived using formula (1) from distributions for 13 THz measured for different temperatures.

measured distributions suggest that *ca.* 200 K below T_N an additional contribution to the inelastic neutron scattering starts to appear and that its origin is different from spin waves.

This work was partly supported by the "Human Capital and Mobility Access to Large Scale Facilities PECO Extention" Program (contract No. ERB CIPD CT 940080).

References

[1] S.H. Liu, *Phys. Rev. B* **2**, 2664 (1970).

[2] H. Sato, K. Maki, *Int. J. Magnetism* **6**, 183 (1974).

[3] J.A. Fernandez-Baca, M.E. Hagen, R.M. Nicklow, T.G. Perring, Y. Tsunoda, *J. Appl. Phys.* **73**, 6548 (1993).

[4] A. Yazaki, K. Tajima, Y. Todate, S. Tomiyoshi, H. Ikeda, *J. Phys. Soc. Jpn.* **63**, 748 (1994).